A Random Walk

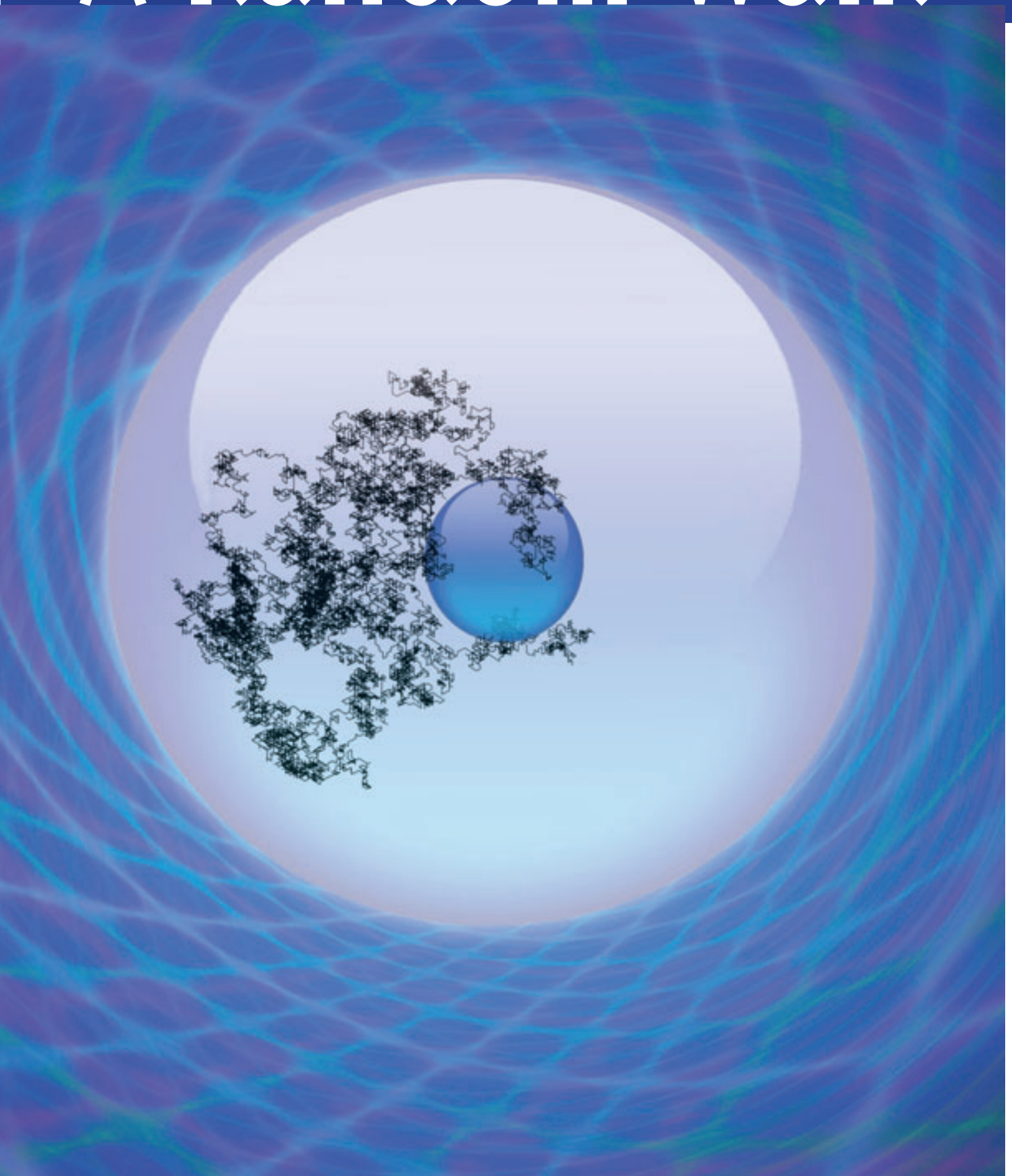

through Electron-Transfer Kinetics

Ryan J. White
Henry S. White
University of Utah

Simulating the random motion of molecules at an electrode can help determine when an electrochemical reaction becomes kinetically controlled.

In common electrochemical usage, a "kinetically controlled reaction" is one in which the transport of redox molecules is fast relative to the rate of electron transfer at the electrode–electrolyte interface. Increasing diffusion rates to reach the kinetic limit is a central concept of many electroanalytical techniques used to investigate electron-transfer kinetics (*1*, *2*). For example, in cyclic voltammetry experiments of freely diffusing redox species, the electrode reaction rate becomes controlled by electron-transfer kinetics at sufficiently high potential sweep rates, a consequence of increased diffusion rates as the sweep rate is increased (*3*–*5*).

In this article, we discuss the role of collisional encounters between the redox molecule and electrode in determining when an electrochemical reaction becomes kinetically controlled. Brownian dynamics simulations of the random motion of redox molecules provide insights into the physical factors that determine the kinetic limit in steady-state voltammetric measurements using electrodes with nanometer dimensions.

Electron transfer at nanoscale electrodes

Reducing the electrode size increases the diffusion-controlled transport rate in steady-state voltammetric measurements. Eventually, the diffusion rate becomes so large that the reaction is limited by electron-transfer kinetics. Several groups, including ours, have used this approach to measure the rate constants of very fast redox reactions (*6*–*8*). Consider the simple electron-transfer reaction $Ox + e^- = Red$ occurring at a spherical electrode of radius a, as shown in Figure 1a. Diffusion of Ox to the electrode surface occurs before the electron-transfer step, and either step may be rate-limiting. At steady state, the rate constant for diffusion (cm/s) of redox molecules to the spherical electrode is simply D/a, in which D is the diffusion constant (cm^2/s) of Ox. Smoluchowski originally used this diffusion rate constant in developing the theory of diffusion-controlled rates of chemical reactions in solution (*9*).

The overall rate of the electrode reaction is partially controlled by the interfacial electron-transfer step when D/a is comparable to or significantly larger than the standard electron-transfer rate constant k_{et} (cm/s)

$$D/a \geq k_{et} \qquad (1)$$

Over the past decade, several research groups have reported the fabrication of platinum electrodes (disk or quasihemisphere geometry) with radii as small as 10 nm (*6*–*12*). If we assume a typical value for D ($\sim 10^{-5}$ cm^2/s) for redox molecules in liquid solutions, D/a at such small electrodes is ~10 cm/s. Thus, in principle, it is possible to use these electrodes, in steady-state voltammetric experiments, to measure values of k_{et} of similar magnitude.

For example, Figure 1b shows a plot of the shift in steady-state voltammetric half-wave potential $\Delta E_{1/2}$, relative to the re-

versible thermodynamic redox potential for the oxidation of ferrocenylmethyltrimethylammonium ($TMAFc^+$) in an H_2O/0.2-M KCl solution. Theoretically, $\Delta E_{1/2}$ is 0 if the reaction is diffusion-controlled, that is, $D/a < k_{et}$. As the electrode radius is reduced to smaller values, a situation is reached in which $D/a \geq k_{et}$. At this point, $\Delta E_{1/2}$ is predicted to increase with decreasing a. The transition between these two regimes is clearly seen in the experimental plot of $\Delta E_{1/2}$ versus log a, occurring at electrode radii <~100 nm. The standard heterogeneous rate constant k_{et} is estimated to be ~5 cm/s by fitting a classical Butler–Volmer rate expression to the data (*6*). The value ~5 cm/s is among the largest reliable values of k_{et} reported in the literature.

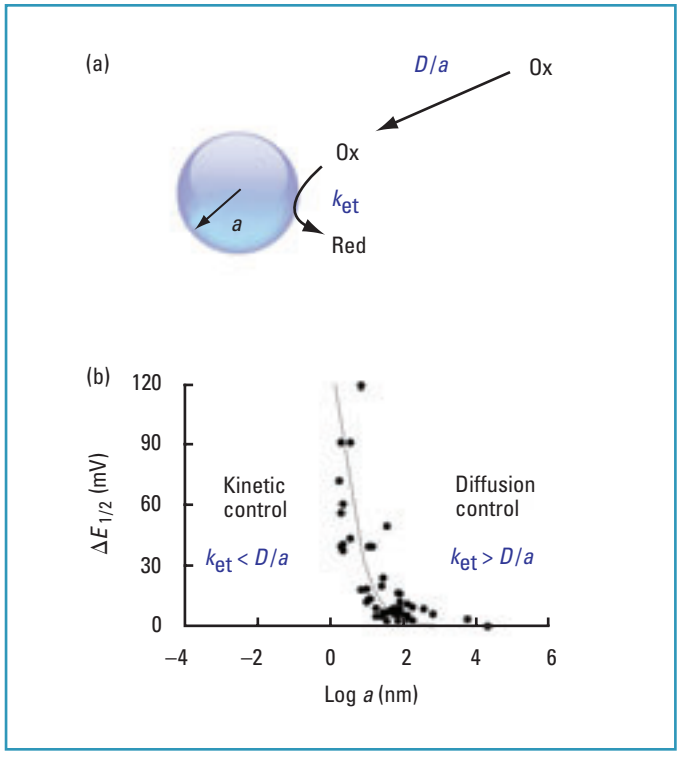

FIGURE 1. Diffusion versus electron-transfer control.

(a) Schematic of the sequential nature of diffusion and electron transfer at a spherical electrode. D/a and k_{et} are the diffusion and electron-transfer rate constants, respectively. (b) Dependence of $\Delta E_{1/2}$ on log a for the oxidation of $TMAFc^+$ in an H_2O/0.2-M KCl solution. Quasihemispherical platinum nanoscale electrodes were used to obtain the data, which illustrate the change from diffusion control to kinetic control as the electrode size is reduced. The dotted line corresponds to a Butler–Volmer kinetic rate expression for k_{et} = 5 cm/s (*6*).

Although Equation 1 is useful in predicting the onset of kinetic control, its physical interpretation is somewhat paradoxical. When an electrode reaction is controlled by electron-transfer kinetics, that is, $D/a > k_{et}$, the rate of the electron-transfer reaction is determined by the collision frequency of redox molecules with the electrode surface and the probability of electron transfer per collision. Because the probability of electron transfer per collision is independent of the electrode size, the observed dependence of the electron-transfer rate on electrode size (i.e., the increase in $\Delta E_{1/2}$ for $TMAFc^+$ oxidation with decreasing a; Figure 1) is solely a consequence of the decreased number of collisional encounters between the redox molecules and the electrode surface. This is intuitively correct: The smaller the electrode, the less frequently a collision occurs between the redox molecules and the electrode. However, collisions between redox molecules and the electrode result from the random, thermally induced motion of the molecules in solution. Thus, collisional encounters (which govern the electron-transfer rate) and diffusion (which governs the transport rate) result from the identical physical process of random molecular motion.

The motion of a redox molecule near an electrode

Three-dimensional Brownian dynamics simulations of the random motion of a redox molecule, as shown on p 214 A, are especially useful in addressing the issue of collision and diffusion rates at nanometer-size electrodes. In these simulations, a spherical electrode of radius a is enclosed in a finite spherical volume of solution that contains a single redox molecule. Although the symmetry of the spherical electrode simplifies the simulations, the conclusions drawn also apply to a hemispherical electrode, which is a good approximation of the geometry of the real nanoscale electrodes used to collect the data in Figure 1.

The initial position of the molecule is randomly chosen to start the simulation. After each time step τ (s), the molecule is allowed to step a distance $\pm\delta$ (cm) in each of the x, y, and z directions. When the molecule hits either the electrode surface or the solution boundary, it is reflected back to its previous position in the following time step. The diffusion coefficient of the molecule is defined by the Einstein relationship $D = \delta^2/2\tau$ (*13*, *14*). This definition of D is consistent with a 3-D random walk, where the net displacement $r = (\delta_x^2 + \delta_y^2 + \delta_z^2)^{1/2}$ for uncorrelated motion in the x, y, and z directions after a time t is given by $r^2 = 6Dt$.

The simulation yields both the collision and diffusion rates of the molecule at the nanoscale electrode. The collision rate is calculated by counting the number of times that the molecule collides with the electrode, then dividing by the total simulation time. The diffusion rate is equal to the number of round-trips that the redox molecule makes between the electrode and the outer solution boundary during the simulation. The collision and diffusion fluxes (both molecules/cm^2s) are computed by dividing the corresponding rates by the area of the electrode.

The trajectory shown on p 214 A corresponds to 20,000 steps between a 20-nm-radius electrode bound by a 100-nm-radius volume of solution. For the purpose of demonstration, τ = 0.5 ns and δ = 1 nm, corresponding to $D = \delta^2/2\tau = 10^{-5}$ cm^2/s. Although these values of τ and δ are unrealistically large for real molecular motion, we will show how the conclusions drawn from these simulations can be applied to any set of τ, δ, and D values.

In this particular simulation, the molecule touches the electrode surface 89 times while making 3 round-trips between the electrode and the exterior surface of the solution. Obviously, different trajectories are obtained each time the simulation is run. However, the trajectory demonstrates the key principle of diffusion and collision that is important in understanding the use of microelectrodes in kinetic measurements: The random-walk nature of diffusion causes the molecule to explore small regions of space very thoroughly before wandering off. Thus, when a redox molecule arrives at the electrode surface, after diffusing in from a far-off distance, it will make many colli-

sions with the electrode before wandering back into the bulk solution. In other words, a redox molecule has many opportunities to accept or donate an electron each time it is in the vicinity of the electrode. We repeated this simulation 1000 times (each trial containing 1 million steps) to obtain average values of $(1.0 \pm 0.2) \times 10^6$ collisions/s and $(6.5 \pm 0.5) \times 10^4$ round-trips/s. Thus, on average, the molecule has ~15 opportunities to undergo electron transfer during each round-trip.

This idea can be more quantitatively expressed by computing the probability that the molecule will collide with the electrode before wandering away. If a molecule is arbitrarily released in solution at a distance b from the center of the electrode, and the radius of the volume boundary is c, then the probability that the molecule will first collide with the electrode before wandering to the outer boundary is (*15*)

$$P_c(b) = a(c - b)/b(c - a) \qquad (2)$$

Equation 2 is readily derived from the ratio of the inward ($b \rightarrow a$) and outward ($b \rightarrow c$) steady-state diffusion rates ($4\pi CDN_A[ac/(c-a)]/4\pi CDN_A[bc/(c-b)]$), in which N_A is Avogadro's number and C is the concentration of the redox molecule (*15*).

Figure 2 shows the results of $P_c(b)$ obtained by Brownian dynamics simulations for the 20-nm-radius electrode contained within the 100-nm-radius spherical solution volume. The dashed line corresponds to the theoretical expectation. In addition to testing the accuracy of our simulation, the results demonstrate the key property of the redox molecule's motion: When the molecule is in the vicinity of the electrode, it has a high probability of colliding with the electrode. Because the redox molecule is in very close proximity to the electrode surface after the first collision, the probability of many additional collisions before it escapes back to the bulk of the solution is very large.

For large values of c, Equation 2 approximates the behavior of a molecule diffusing at a real nanoscale electrode immersed in a semi-infinite volume of solution. In the limit $c \rightarrow \infty$, Equation 2 reduces to $P_c(b) = a/b$, which is plotted as the solid line in Figure 2. The plot indicates that the simulation of a finite-volume solution yields reasonable predictions of $P_c(b)$ for the semi-infinite system, especially when the molecule is released very close to the electrode surface. This approximation is used below in determining the reversibility of the electrode reaction.

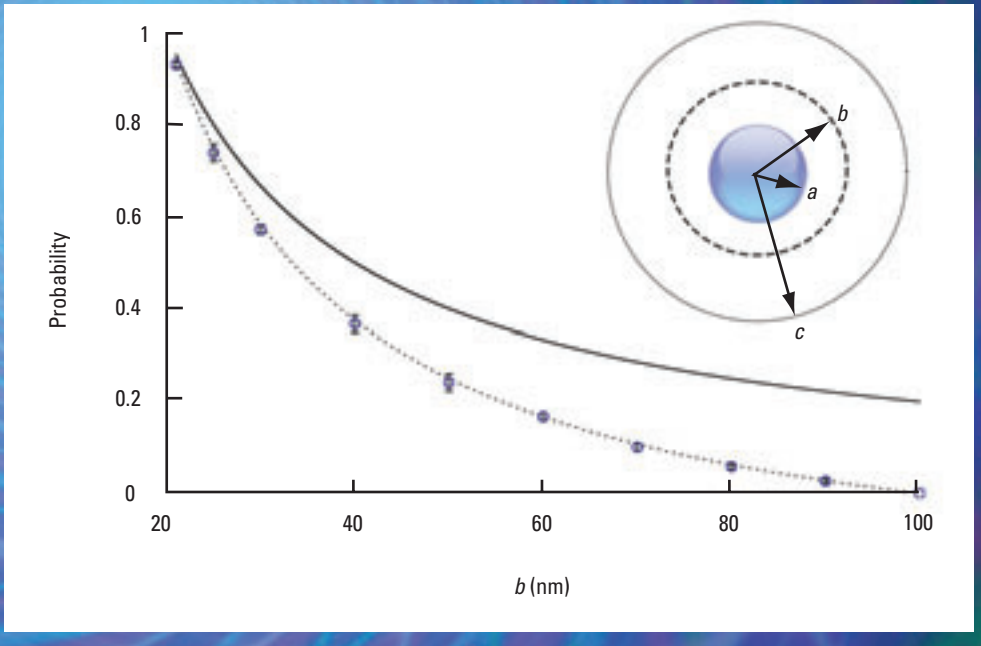

FIGURE 2. Molecular encounters with the electrode.

A plot of the probability of a molecule encountering a 20-nm-radius electrode when released at a distance b from the center of the electrode before diffusing away to a distance of 100 nm. The dashed line plots the theoretical expectation when a = 20 nm and c = 100 nm. The solid line represents $P_c(b)$ when $c \rightarrow \infty$ (i.e., an electrode in a semi-infinite solution).

Diffusion and collision rates

The diffusion-limited transport rate of the molecule can be computed by counting the number of round-trips the molecule makes during the simulation. This is most easily understood by arbitrarily designating the electrode as the anode and the outer solution boundary as the cathode. When the molecule collides with the electrode surface, we assume that it is oxidized with unit probability. It remains oxidized, regardless of further collisions with the electrode, until it returns to the outer solution boundary where it is reduced with unit probability. Thus, one round-trip, or one redox cycle with single oxidation and reduction events, generates one electron in a wire connected to the electrodes.

We simulated the round-trip transport by using a range of simulation step lengths (τ = 0.25–2.0 nm) and step times (δ = 0.0313–0.5 ns) while maintaining a constant $D = 10^{-5}$ cm^2/s. Transport rates depend on D but are independent of the specific values of δ and τ used to define D. The rate of diffusive transport R (s^{-1}) of a molecule between two concentric spheres, easily derived from Fick's laws of diffusion, is $R = 4\pi CDN_A[ac/(c - a)]$. We checked our simulation by computing R for a single molecule confined between a 50-nm-radius electrode and a 100-nm-radius outer boundary (corresponding to $C = 4.52 \times 10^{-10}$ mol/cm^3). The transport rate obtained by simulation of the molecule's motion for 0.5 ms [$(3.1 \pm 0.5) \times 10^5$ s^{-1}] is in good agreement with the analytical expression (3.4×10^5 s^{-1}).

To help visualize the origin of the kinetic limit at small electrodes, Figures 3a and 3b present plots of the collisional flux Ω (molecule/cm^{2}s), normalized to the diffusive flux, of molecules as a function of the electrode size. Values of Ω were computed by counting the number of collisions during a simulation and dividing by the simulation run time and the electrode area. In plot-

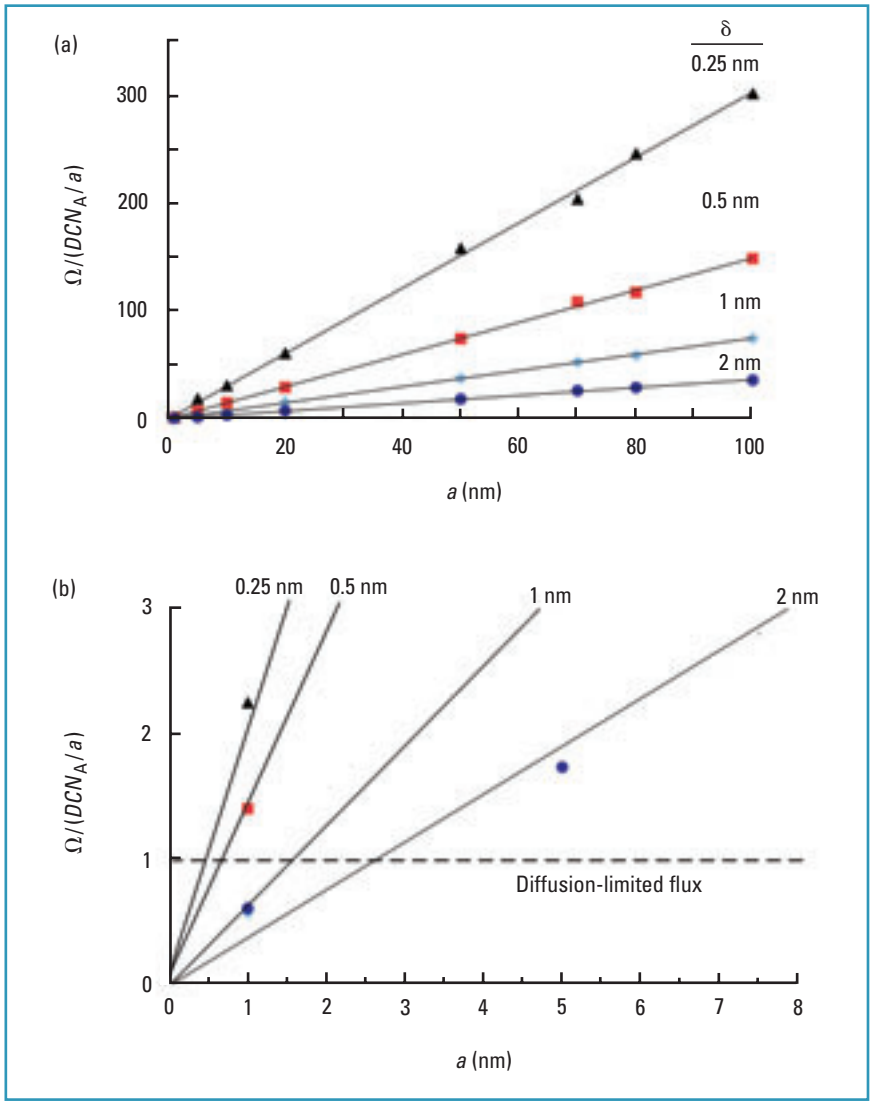

FIGURE 3. Collisional flux.

(a) Normalized Ω/J, in which $J = DCN_A/a$, as a function of the electrode radius and δ. (b) Enlarged region of (a) for $a \rightarrow 0$. The dashed line represents the normalized diffusion-limited flux ($J/J = 1$) and corresponds to instantaneous electron transfer upon collision. The solid lines represent least-squares regressions for each data set.

ting Figure 3, we normalized Ω to the diffusion-limited flux $J = DCN_A/a$ at a spherical electrode. Thus, these results apply to any value of D, C, or a. J is a function of D, which as noted above, is independent of the specific values of δ and τ that define D. However, Ω depends on D as well as the choice of the microscopic parameter δ, or equivalently, τ. Thus, the family of curves in Figure 3 corresponds to various values of δ. The horizontal dashed line in Figure 3b corresponds to the normalized diffusion-limited flux ($J/J = 1$) that would be observed if electron transfer occurred with unity probability during each collision.

Before we can describe how Figure 3 is used to understand the origin of the kinetic limit, it is first necessary to appreciate why the collisional rate depends on δ, whereas the diffusion rate, which depends on D, is not a function of δ. The collisional rate depends on δ (while maintaining constant D) because the molecule tends to explore the space around it more thoroughly when δ is smaller. Thus, a molecule near the electrode surface with a smaller δ will tend to collide with the electrode more frequently.

This result was already encountered in Figure 2, which indicated that the probability of collision with the electrode surface, $P_c(b) \approx a/b$, decreased as the initial distance of the molecule from the electrode increased. Thus, if we identify δ in the simulation as also being equal to the closest distance that the molecule approaches the surface and substitute $(a + \delta)$ for b in $P_c(b) = a/b$, we obtain the dependence of the probability of collision on δ, $P_c(a + \delta) = a/(a + \delta)$. The conclusion is clear: Smaller values of δ result in a higher likelihood of a collision with the electrode before the molecule wanders off to the bulk solution. In other words, the collision frequency is a function of δ. As the electrode size is made smaller and smaller, $a/\delta \rightarrow 0$ and $P_c(a + \delta) \rightarrow a/\delta$.

How many collisions are required?

Kinetic control in an electrochemical reaction occurs when the collisional rate becomes smaller than the diffusion-limited rate. This transition is located at the intersection of the normalized diffusion-controlled (dashed) and the collision flux lines (solid) in Figure 3b. From the simulations, Ω increases in inverse proportion to δ. Thus, δ is the critical kinetic parameter that determines when the kinetic limit is reached. It is instructive to ask how δ is related to k_{et}, which is often used as the kinetic metric in electrochemistry. The relationship between these parameters is obtained by noting that $k_{et} = \nu P_{et}$, in which ν is the velocity of the redox molecule and P_{et} is the probability of electron transfer upon a single collision with the electrode surface. By definition, molecular velocity in the computer simulation is equal to δ/τ. Combining this with $D = \delta^2/2\tau$ provides the relationship between ν and δ: $\nu/2D = \delta^{-1}$. To demonstrate that the Brownian dynamics simulations are consistent with these relationships between D, ν, and δ, we computed the velocity by noting that Ω is simply equal to νC (*16*). In Figure 4, values of ν obtained from the simulation (normalized to $2D$ to make the results universal for any value of D) are plotted versus δ^{-1} and are compared to the theoretical expectation $\nu/2D = \delta^{-1}$ (dashed line).

The relationship between k_{et} and δ can now be obtained by substituting $\nu/2D = \delta^{-1}$ into $k_{et} = \nu P_{et}$. The result is

$$k_{et} = (2D/\delta)P_{et} \qquad (3)$$

If we assume unit probability for electron transfer ($P_{et} = 1$), then the upper limit for the electron-transfer rate constant for a freely diffusing species is $k_{et}^{max} = 2D/\delta$. Because values of D

are readily measured, evaluating k_{et}^{max} only requires knowing δ. In the computer simulations presented earlier, δ is specified. For example, the curve labeled δ = 1 nm in Figure 3b corresponds to k_{et}^{max} = 200 cm/s, again assuming $D = 10^{-5}$ cm^2/s.

In real chemical systems, it is difficult to assign a precise numerical value to δ because molecules do not jump precise distances during a predetermined discrete time step (*17*). Furthermore, the random motion of molecules as they collide with their neighbors does not lend itself to being described by a well-defined velocity, as discussed by Einstein and Berg (*14*, *15*, *18*). However, the root-mean-square thermal velocity, $\langle v^2 \rangle^{1/2} = (kT/m)^{1/2}$ (in which k is Boltzmann's constant, T is absolute temperature, and m is the mass of an individual molecule), has been previously used to estimate k_{et}^{max} (*16*, *19*). It is interesting to explore this approach in considering electron-transfer reactions at very small electrodes.

For $TMAFc^+$, which was used to obtain the experimental data in Figure 1, $m = 4.05 \times 10^{-22}$ g and $\langle v^2 \rangle^{1/2} = 1.0 \times 10^4$ cm/s. If we recall that k_{et} = ~5 cm/s for oxidation of $TMAFc^+$ and accept that 1.0×10^4 cm/s is the "true molecular velocity", then $P_{et} = k_{et}/k_{et}^{max} = 0.0005$. In other words, the experimental evidence suggests that the oxidation of $TMAFc^+$ involves, on average, 2000 collisional encounters with the electrode before an electron-transfer event occurs. Note that the oxidation of $TMAFc^+$ is a very fast reaction. Reactions with smaller k_{et} require many more encounters to proceed at a significant rate.

The low probability of electron transfer during each molecule–electrode encounter has interesting implications when we consider steady-state voltammetry at a nanoscale electrode. First, note that $\langle v^2 \rangle^{1/2} = 1.0 \times 10^4$ cm/s corresponds to δ = 0.02 nm for $D = 10^{-5}$ cm^2/s. This value of δ is 50× smaller than that used in the simulation on p 214 A to compute the rates of collision and transport at a 20-nm-radius electrode (1×10^6 collisions/s and 6.5×10^4 round-trips/s, respectively). Thus, because the collision rate is inversely proportional to δ, a velocity of 1.0×10^4 cm/s corresponds to a collision rate of 50×10^6 s^{-1} at a 20-nm-radius electrode. The diffusion rate is independent of δ, so the number of round-trips per second, 6.5×10^4, remains constant. Therefore, there are $(50 \times 10^6$ collision/s)/$(6.5 \times 10^4$ round-trips/s) ≈ 770 collisions/round-trip. Because a successful electron-transfer event for k_{et} = 5 cm/s requires 2000 collisions, this implies that only 1 out of every 2.5 molecules of $TMAFc^+$ that diffuse to the electrode actually undergoes electron transfer at a 20-nm-radius electrode. The reaction is thus controlled partially by diffusion and electron transfer.

In electrochemical terminology, this scenario corresponds to a quasireversible reaction. If we were to reduce the electrode radius by a factor of 5 to 4 nm, only 1 out of every 75 collisions would result in an electron transfer, and the reaction would be considered irreversible. A factor of 5 increase in the radius to 100 nm would result in 20,000 collisions per $TMAFc^+$ that diffuses to the electrode, far more than is required for electron transfer (~2000 collisions). This scenario corresponds to a reversible electron-transfer reaction. Interpretation of the reversibility in terms of the number of collisions is reflected by the onset of a shift in $E_{1/2}$ in the experimental data (Figure 1b) when the electrode radius is reduced below 100 nm.

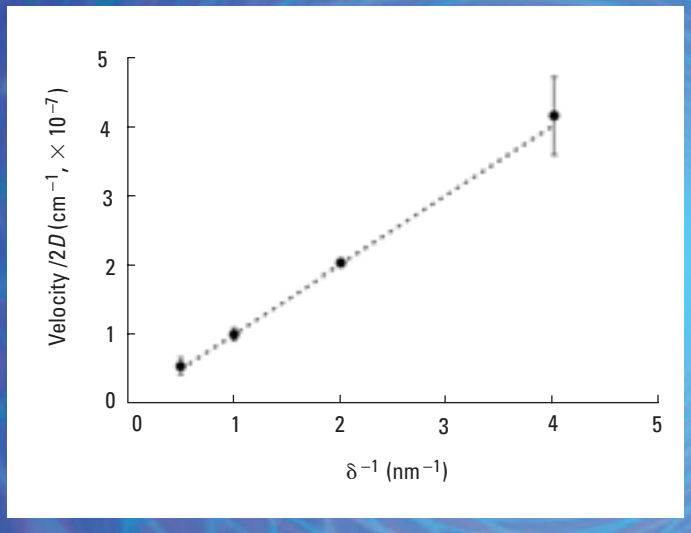

FIGURE 4. Redox molecule velocity.

A plot of the normalized "molecule velocity", $v/2D$, as a function of δ^{-1}. The data correspond to values of the velocity computed from collisional flux values obtained by computer simulation. The dashed line corresponds to the theoretical expectation ($v/2D = \delta^{-1}$), based on the definitions of the instantaneous molecule velocity ($v = \delta/\tau$) and the diffusion coefficient ($D = \delta^2/2\tau$).

These estimates of the probability of electron transfer per collision assume $\langle v^2 \rangle^{1/2} = 1.0 \times 10^4$ cm/s and $D = 10^{-5}$ cm^2/s, which correspond to δ = 0.02 nm and τ = 0.2 ps. These latter values are consistent with realistic length and time scales that we might anticipate for a random walk of a redox molecule through the solution (*17*). However, one must ask whether these values really describe the dynamics of random motion that are important as the redox molecule approaches the electrode surface. For example, there is evidence that the solution viscosity at the solid–liquid interfaces is slightly lower than that of the bulk solution and that this may change the effective diffusivity of the molecule as it approaches the electrode surface (*20*, *21*). In addition, our results assume that the redox molecules are freely diffusing and are not influenced by the electric field that extends from the charged electrode surface (*22–26*). Migration of charged molecules in large electric fields can potentially alter the redox distributions, fluxes, and driving force for electron-transfer reactions at nanoscale electrodes (or in ultrafast scan voltammetry). For example, electrical double-layer effects are readily evident in the oxidation of $IrCl_6^{3-}$ at platinum electrodes with radii <50 nm (*27*).

In addition to those factors, we have implicitly assumed that the collision frequency reflects the diffusion motion of the molecule as it intercepts the electrode–solution interface. An alternative formulation of the collision frequency is based on the

concept of an encounter pre-equilibrium complex, in which the effective collision frequency reflects the frequency of surmounting the free energy barrier for electron transfer after the redox molecule arrives at the interface. The pre-equilibrium model predicts encounter frequencies that are approximately an order of magnitude larger than values based on random diffusive molecular motion. An excellent comparison of these models has been presented by Hupp and Weaver (*28*).

We have also made the assumption in our simulations that the redox molecule needs to "touch" the electrode for electron transfer to occur. Kinetic measurements of redox molecules attached to metal surfaces with well-defined molecular spacers have clearly demonstrated the likelihood of long-range electron transfer in reactions involving fast outer-sphere redox (*29*). Furthermore, the rate of tunneling between the electrode and the redox molecule is distance-dependent (*29*). These additional factors are required in future computational models of electron-transfer reactions that involve freely diffusing redox species.

Reinterpreting the criterion $D/a > k_{et}$

We conclude by returning to the meaning of the phrase "kinetically controlled reaction" used in electrochemistry. From a purely pragmatic point of view, the commonly used criterion for kinetic control in steady-state voltammetric measurements (i.e., $D/a > k_{et}$) is very useful for experimentalists because D, a, and k_{et} are all readily measurable values. However, we have shown that the magnitude of k_{et}^{max} (and thus of k_{et}) is also related to D. The dependence of the kinetic criterion on D can be eliminated altogether by substituting $k_{et} = (2D/\delta)P_{et}$ into Equation 1, yielding the simple dimensionless relationship $\delta/a > 2P_{et}$. As we have seen, in the limit $a \rightarrow 0$, the left-hand side of this expression is simply the inverse of the probability that the molecule hits the surface, $P_c = a/\delta$. Thus, the criterion for kinetic control can be written as

$$P_c P_{et} < 0.5 \qquad (4)$$

This expression has a very simple physical interpretation: The electrochemical reaction is kinetically controlled when either the encounter frequency or the success rate of electron transfer per encounter is small. This conclusion is precisely the intuitive result.

The electrochemical reaction is kinetically controlled when either the encounter frequency or the success rate of electron transfer per encounter is small.

We thank Joel M. Harris for enlightening comments on the role of random walks in reaction kinetics. This work was supported in part by the Office of Naval Research, the Department of Defense Multidisciplinary University Research Initiative (MURI) program administered by the Office of Naval Research under Grant N00014-01-1-0757, and the Defense Advanced Research Project Agency.

Ryan J. White is a Ph.D. student in the department of chemistry at the University of Utah. His thesis focuses on stochastic detection of particles with nanopore sensors. Henry S. White is a professor at the University of Utah. His research interests focus on electrochemistry. Address correspondence about this article to him at white@chem.utah.edu.

References

(1) Bard, A. J.; Faulkner, L. R. *Electrochemical Methods*, 2nd ed.; Wiley & Sons: New York, 2001.
(2) Girault, H. H. *Analytical and Physical Electrochemistry*; Marcel Dekker: New York, 2004.
(3) Wipf, D. O.; et al. *Anal. Chem.* **1988**, *60*, 306–310.
(4) Hseuh, C.; Brajter-Toth, A. *Anal. Chem.* **1993**, *65*, 1570–1575.
(5) Amatore, C.; Maisonhaute, E.; Simmonneau, G. *J. Electroanal. Chem.* **2000**, *486*, 141–155.
(6) Watkins, J. J.; et al. *Anal. Chem.* **2003**, *75*, 3962–3971.
(7) Penner, R. M.; et al. *Science* **1990**, *250*, 1118–1121.
(8) Chen, S.; Kucernak, A. *J. Phys. Chem. B* **2002**, *106*, 9396–9404.
(9) Gardiner, W. C. *Rates and Mechanisms of Chemical Reactions*; Benjamin/Cummings Publishing: Menlo Park, CA, 1969.
(10) Shao, Y.; et al. *Anal. Chem.* **1997**, *69*, 1627–1634.
(11) Slevin, C. J.; et al. *Electrochem. Commun.* **1999**, *1*, 282–288.
(12) Pendley, B. D.; Abruña, H. D. *Anal. Chem.* **1990**, *62*, 782–784.
(13) Einstein, A. *Ann. Phys.* **1905**, *17*, 549–560.
(14) English translations of Refs. 13 and 18: Einstein A. *Investigations on the Theory of the Brownian Movement*; Dover Publications: Mineola, NY, 1956.
(15) Berg, H. C. *Random Walks in Biology*; Princeton University Press: Princeton, NJ, 1983.
(16) Andersen, O. S.; Feldberg, S. W. *J. Phys. Chem.* **1996**, *100*, 4622–4629.
(17) Glasstone, S.; Laidler, K. J., Eyring, H. *The Theory of Rate Processes*; McGraw-Hill: New York, 1941.
(18) Einstein, A. *Z. Elektrochem.* **1907**, *13*, 41–42.
(19) Marcus, R. *J. Chem. Phys.* **1965**, *43*, 679–701.
(20) Morris, R. B.; Franta, D. J.; White, H. S. *J. Phys. Chem.* **1987**, *91*, 3559–3564.
(21) Seibold, J. D.; Scott, E. R.; White, H. S. *J. Electroanal. Chem.* **1989**, *264*, 281–289.
(22) Watkins, J. J.; Zhang, B.; White, H. S. *J. Chem. Educ.*, **2005**, *82*, 712–719.
(23) Norton, J. D.; White, H. S.; Feldberg, S. W. *J. Phys. Chem.* **1990**, *94*, 6772–6780.
(24) Smith, C. P.; White, H. S. *Anal. Chem.* **1993**, *65*, 3343–3353.
(25) Amatore, C.; Lefrou, C. *J. Electroanal. Chem.* **1990**, *296*, 335–358.
(26) Grün, F.; et al. *J. Chem. Phys.* **2004**, *120*, 9648–9655.
(27) Watkins, J. J.; White, H. S. *Langmuir* **2004**, *20*, 5474–5483.
(28) Hupp, J. T.; Weaver, M. J. *J. Electroanal. Chem.* **1983**, *152*, 1–14.
(29) Smalley, J. F.; et al. *J. Phys. Chem.* **1995**, *99*, 13,141–13,149.